Model for Indefinitely Rising Regge Trajectories*

U. TRIVEDI
California Institute of Technology, Pasadena, California 91109
(Received 17 July 1969)

The model for indefinitely rising Regge trajectories is based on the l-excitation scheme. It has been suggested that the effective strength of forces due to Regge-trajectory exchanges increases with energy in order to overcome the centrifugal repulsion. The output Regge trajectory is thus pulled up with energy. The suggested energy increase is simulated in a simple manner by considering a Yukawa potential with an energy-dependent coupling strength. It is found therein that the output trajectory must grow at least as fast as $\sqrt{s}$. Furthermore, accompanying the leading trajectory there occurs an infinite set of trajectories associated with higher radial quantum numbers. Trajectories characterized by finite radial quantum numbers are "parallel" to the leading trajectory for large s. The various resonances occur in a well-specified pattern. This pattern has been compared with the nonstrange baryon spectrum and is compatible with it. The behavior of Imα and some multichannel effects on Reα are also discussed.

I. INTRODUCTION

THE dynamical explanation for high-rising Regge trajectories α has brought forth some interesting speculations. For the single-channel Yukawa-potential scattering, the Regge trajectories fall down very rapidly after a few—two or three—particle manifestations. This has led many authors[1] to believe that an explanation for the empirical behavior of trajectories lies in the multichannel nature of the problem. With the Carruthers-Nieto model as a starting point, it has been suggested that Reα is built up not by an addition of orbital angular momenta, the l-excitation scheme, but by an increase in the spin of the internal particles, the orbital angular momenta being kept low in this case. Thus, as the energy increases, it is thought that we are always in the neighborhood of two-body channels formed by particles, one of them at least having a high spin and low l. Such a channel, it is supposed, gives rise to a resonance with high spin and mass. We thus have a set of resonances with increasing spin and mass. It is not clear, however, that this set of resonances arises from the particle mainfestations of a single Regge trajectory. From the dispersion relations for α, though, one sees that a sharp increase of Imα due to the opening of a new channel raises the Reα; successive increases would raise Reα with energy. It is thus conceivable that the set of resonances mentioned above do lie on the same trajectory. In the present paper, we consider the opposite point of view, namely, that the increase in Reα is primarily due to the increasing orbital angular momenta in a single channel, and present the consequences of such a scheme. Multichannel effects are supposed to be small, and are taken into account while discussing Imα or Γ_{tot}.

To develop our ideas, we focus on the nucleon trajectory and the Δ trajectory. Singh and Udgaonkar[2] have shown within the static-model formalism for the πN single channel that $I=\frac{3}{2}$, $J=l+\frac{1}{2}$ and $I=\frac{1}{2}$, $J=l-\frac{1}{2}$, odd l, reciprocally bootstrap to a very good degree, and that the forces in $I=\frac{3}{2}$, $J=l-\frac{1}{2}$ and $I=\frac{1}{2}$, $J=l+\frac{1}{2}$, odd l, are weak. Our first concern is to formulate the above bootstrap of the nucleon trajectory and the Δ trajectory in a nonstatic language.

The classic example of the l-excitation scheme is, of course, the radial Schrödinger equation. We rely heavily on such a differential equation to provide the nonstatic language as well as the dynamical expectations. Let us consider the differential equation

$$\frac{d^2\psi_I{}^{\pm}}{dr^2}+\left[q^2+V_I{}^{\pm}-\frac{l(l+1)}{r^2}\right]\psi_I{}^{\pm}=0, \qquad (1.1)$$

$(+)\equiv$positive signature, $(-)\equiv$negative signature, $I\equiv$isospin of s channel,

$$q^2=[s-(m+\mu)^2][s-(m-\mu)^2]/4s,$$

and $J=l\pm\frac{1}{2}$, where the symbols have their usual meaning. In the above, $V^{\pm}$ represents an equivalent potential

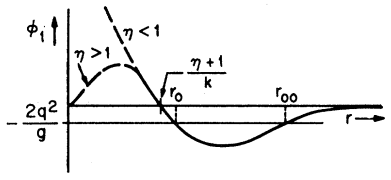

FIG. 1. Illustration of the condition which q^2/g has to fulfill in order to produce the maximum r_0 and minimum r_{00} of $\phi(r)$.

* Work supported in part by the U. S. Atomic Energy Commission, under Contract No. AT(11-1)-68, of the San Francisco Operations Office, U. S. Atomic Energy Commission.

[1] P. Carruthers and M. M. Nieto, Phys. Rev. **163**, 1646 (1967); E. Golowich, *ibid.* **158**, 1745 (1968); S. Y. Chu and C. I. Tan, University of California Radiation Laboratory Report No. UCRL-17511, 1967 (unpublished); S. Mandelstam, *Elementary Particle Physics* (W. A. Benjamin, Inc., New York, 1967), Part II, p. 1.

[2] See, for instance, B. M. Udgaonkar, *High Energy Physics and Elementary Particles* (International Atomic Energy Agency, Vienna, 1965), p. 791. The neglect of t-channel exchanges in this model may be considered as a first approximation. It may turn out ultimately that t-channel exchanges are not perturbative. But even in this situation the u-channel exchanges must play an important role since the $\Delta J=2$ rule is true for the empirically observed baryon Regge trajectories. In any event, we regard this model as a motivation for the general dynamical scheme outlined subsequently.

arising from the exchange of Regge trajectories in the t and u channels.[3]

We now incorporate the results of the static model in terms of the above symbols and focus our attention on the $I=\frac{3}{2}$ states of the s channel. First, it is required that for

$$I=\tfrac{3}{2},\quad J=l+\tfrac{1}{2},\quad \text{negative signature},\quad V_{3/2}{}^{-}>0. \tag{1.2}$$

Since in the static model the dominant force in the $I=\frac{3}{2}$, $J=l+\frac{1}{2}$, l odd, states arises from the nucleon-trajectory exchange, we have for

$$I=\tfrac{3}{2},\quad J=l+\tfrac{1}{2},\quad V_{3/2}{}^{\mp}\simeq\pm\sum_{n\ \text{odd}} V_{3/2}(I=\tfrac{1}{2},n), \tag{1.3}$$

under the sharp-resonance approximation for the exchanged nucleon trajectory. In (1.3), the term $V_{3/2}(I=\frac{1}{2},n)$ refers to the effective potential arising from the exchange of an $I=\frac{1}{2}$, $J_n=n-\frac{1}{2}$, n odd, $m_n{}^2\approx(J_n-a)/b$ particle, in the $I=\frac{3}{2}$, $J=l+\frac{1}{2}$, s-channel states.

The dynamical picture of the static model now implies that $V_{3/2}(I=\frac{1}{2},n)$ is the dominant element when $s\approx(J-a')/b'$, $J=l+\frac{1}{2}$, $l=n$, n odd, and that it gives rise to sufficient attraction to form a resonance. It is clear as to what this means; in (1.3), $V_{3/2}{}^{-}$ is an energy-dependent equivalent potential whose strength increases with energy. The increase in strength overcomes the repulsion for high l in the region $r\approx 1/m_n$ and gives rise to a resonance. The Reα for the Δ trajectory is thus pulled up with energy.

We now point to a major consequence resulting from the above assumptions. Evidently if $V_{3/2}{}^{-}\approx V_{3/2}\times(I=\frac{1}{2},n)$ yields sufficient attraction to form a resonance with $J=l+\frac{1}{2}$, $l=n$, $s\approx(J-a')/b'$, it must also form resonances in the lower partial waves $l=n-1$, $n-2$, $\cdots$, 1, 0 for energies in the neighborhood of interest. Thus, in explaining the leading Δ trajectory, we obtain an infinite number of accompanying trajectories with $I=\frac{3}{2}$, separated by roughly an integer. Within our framework, the interpretation is clear; the leading Δ trajectory corresponds to resonances whose ψ's have no node in the interaction region, the next lower trajectory to resonances whose ψ's have one node, and so on. We may thus denote the trajectories by α_m, $m=0$, 1, 2, 3, $\cdots$, where m refers to the radial quantum number.

The above argument may be repeated verbatim for the $I=\frac{1}{2}$ states of the s channel with the N-trajectory exchange replaced by the Δ-trajectory exchange. The pattern for the output nucleon trajectories is the same as above with the Δ trajectories replaced by the nucleon trajectories.

The general dynamical scheme that emerges from the above discussion is that the attractive strength of the force arising from Regge-trajectory exchanges increases with energy. The increase in the attraction is sufficient to counteract the repulsion due to high orbital angular momenta associated with a two-particle channel whose internal particles have low spin. The output Regge trajectory could thus rise indefinitely with s. Furthermore, as a consequence of this dynamical scheme, trajectories distinguished by their radial quantum numbers accompany the leading trajectory, separated roughly by a unit from each other. We thus expect such a pattern to be present in the hadron spectrum.

To gain a better understanding of the pattern for Reα_n, as well as the behavior of Imα, we have studied the differential equation (1.1) with

$$V=g(s)e^{-kr}/r,\quad g(s)>0,\quad s\geq s_0>0. \tag{1.4}$$

The coupling strength g is considered to be energy-dependent, monotonically increasing with energy. We thus simulate in a rather simple fashion the suggested increase in strength of the Regge-trajectory-exchange equivalent potential.[4]) The resulting differential equation is studied in Sec. II. It is found therein that

$$\begin{aligned}&\mathrm{Re}\alpha_n\simeq -cn+a+b\sqrt{g},\\ &n=0,\ 1,\ 2,\cdots,<\infty,\quad c=\sqrt{2}\end{aligned} \tag{1.5}$$

[3] L. A. P. Balázs, Phys. Rev. **137**, B1510 (1965); **139**, B1646 (1965); J. Finkelstein, *ibid.* **154**, 1596 (1967); L. Durand III, *ibid.* **166**, 1680 (1968); S. Frautschi and B. Margolis, Nuovo Cimento **56A**, 1155 (1968); S. Frautschi, O. Kofoed-Hansen, and B. Margolis, *ibid.* **61A**, 41 (1969). In the work of Durand, the idea of an equivalent potential representing a Regge-trajectory exchange is implicit. The underlying idea in the works of Frautschi *et al.* also involves the notion of an equivalent potential arising from a Regge-trajectory exchange. However, the use of the eikonal approximation therein requires that dibaryon Regge trajectories do not rise indefinitely. This requires cancellations among the exchanged boson-trajectory potentials so that, for large s, the net force is weak or highly repulsive. Similar cancellations, or repulsions, must also occur in order to avoid the so-called exotic Regge trajectories. The mathematical requirements placed on the exchanged Regge trajectories will be different from those placed by the "duality" idea. It would be of interest to explore their consequences. For example, the static-model generalization to $SU(3)$ (Ref. 2) required the octet and the decuplet (as well as their respective l-excitations among themselves) to be degenerate in mass. In the nonstatic language, this would mean that the octet trajectory is degenerate with respect to the decuplet trajectory. The forces in the exotic representations turn out to be weak in the static model. The static model is perhaps an indication of what one may expect in the nonstatic version of conditions excluding the possibility of exotic Regge trajectories.

[4] The equivalent potentials for unequal-mass spinless external particles are well known. In these cases, a single Regge-trajectory-exchange equivalent potential has the form

$$V(s,r)=\int_{t_1}^{\infty} dt'\ \mathrm{abs}[f_R(s,t')]\frac{e^{-r\sqrt{t'}}}{r},$$

where $f_R(s,t')$ is the Regge-trajectory exchange amplitude. It is clear from this expression that the effective strength of the force is in a sense an average over the various exchanged particles. The residue function and the trajectory function of the exchange determine the variation of $V(s,r)$ with s. The study of this variation, though amenable in principle, is complicated. A rough preliminary numerical calculation with rapidly decreasing Γ_{el} for the spin-zero equal-mass problem suggests that trajectories are indeed pulled up in the manner suggested. We would like to state here that equivalent potentials for unequal-mass spin-zero and spin-$\frac{1}{2}$ external particles have been obtained by us for both $J=l+\frac{1}{2}$ and $J=l-\frac{1}{2}$. They behave like $1/r$ at $r=0$. The generalization to unequal-mass arbitrary-spin external particles is being studied. It is hoped that the $1/r$ behavior at $r=0$ will persist; we have therefore considered an energy-dependent Yukawa potential in our discussion.

provided $q^2/g \simeq s/g \to 0$ as $s \to +\infty$. What is relevant for us is that $0<c<2$, so that utilizing the monotonicity of $g(s)$, we have

$$s_{J_n} < s_{J_{n+1}} < s_{J_{n+2}}, \tag{1.6}$$

where

$$\mathrm{Re}\alpha_n(s_{J_n}) = J,$$
$$\mathrm{Re}\alpha_{n+1}(s_{J_{n+1}}) = J,$$

and

$$\mathrm{Re}\alpha_n(s_{J_{n+2}}) = J+2.$$

We may note that under similar conditions for the square well with depth g, $c>2$, so that the resulting pattern is different although the essential physical picture is the same. In Sec. III, taking $g \approx s^2$ as is suggested empirically, the pattern shown in (1.6) is compared with the positive- and negative-parity spectrum of nonstrange baryons.

In order to understand the empirical behavior of $\mathrm{Im}\alpha$, in other words, Γ_{tot}, we have necessarily to take account of the multichannel nature of the problem. To display the essential physical features involved, we develop a simple multichannel formalism in Sec. IV. The effect of the other channels on the trajectory generated by the single channel is then presented using the dispersion relations satisfied by α.

II. TRAJECTORY FUNCTION FOR LARGE ATTRACTION

In this section[4a] we propose to discuss the Regge trajectories arising from the following differential equation:

$$\frac{d^2\psi}{dr^2} + \left[q^2 + V(s,r) - \frac{\lambda^2 - \frac{1}{4}}{r^2} \right] \psi = 0, \quad \lambda = l + \tfrac{1}{2} \tag{2.1}$$

where

$$\lim_{s\to\infty} \frac{q^2}{s} \approx O(1), \tag{2.2}$$

and where

$$V(s,r) = g(s) e^{-kr}/r. \tag{2.3}$$

In writing $V(s,r)$ as in (2.3), we simulate the short-range character and the energy dependence of the equivalent potential arising from a Regge-trajectory exchange.[4] For the sake of curiosity, in the following we will take

$$V(s,r) = g(s) r^{\eta-1} e^{-kr}, \quad \infty > \eta > -1. \tag{2.4}$$

In our study we adopt the JWKB formalism. We therefore define the square of the "velocity" function

$$Q^2(r) = q^2 + g r^{\eta-1} e^{-kr} - \lambda^2/r^2 = (g/r^2)[\phi(r) - \lambda^2/g], \tag{2.5}$$

where

$$\phi(r) = r^{\eta+1} e^{-kr} + q^2 r^2/g. \tag{2.6}$$

[4a] On completion of this work, Dr. R. Yves informed the author of a work by G. Tiktopoulus [Phys. Letters **29B**, 185 (1969)], where essentially similar ideas have been dealt with. The author is grateful to Dr. R. Yves for drawing his attention to this work.

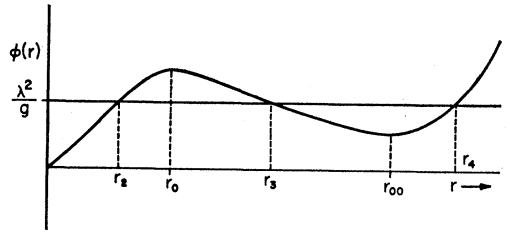

FIG. 2. Illustration of the condition which λ^2/g has to fulfill in order to produce the three classical turning points r_2, r_3, and r_4.

We consider here q^2 and λ real and positive. To begin with, let us suppose that

$$q^2/g \to \infty.$$

In this event the differential equation approaches the "free" form since the effect of the potential becomes negligible. Thus no resonances can be formed and in fact the Regge trajectories recede into the left half λ plane as for the case when g is independent of s. Similarly, we can see that when

$$\lambda^2/g \to \infty,$$

no Regge trajectories occur. This corresponds to the fact that for $V(s,r)$ of the form (2.4) for any finite s, the Regge poles lie in a bounded domain in the right half λ plane.

The behavior discussed above is intimately related with our ability to generate the three classical turning points $r_2<r_3<r_4$, $Q^2(r_i)=0$, $i=2, 3, 4$, with $Q^2(r)>0$ for $r_2<r<r_3$, so that a resonant state may be formed. The function $\phi(r)$ has a maximum and a minimum at r_0 and r_{00} provided (see Fig. 1)

$$0 < 2q^2/g < |(\phi_1)_{\min}|,$$
$$\phi_1 = -\frac{1}{r}\frac{d\phi}{dr} - \frac{2q^2}{g}.$$

It can be easily seen that when

$$q^2/g \to 0, \quad r_0 = (\eta+1)/k + 0, \quad r_{00} \to +\infty, \tag{2.7}$$

this case is of interest to us, as will be evident later. From Fig. 2 we can see that for r_2, r_3, and r_4 to occur, we must have

$$\phi(r_{00}) < \lambda^2/g < \phi(r_0).$$

Let us now consider the situation when

$$\lambda^2/g \nrightarrow \phi(r_0);$$

that is, when

$$(r_3 - r_2) \nrightarrow 0.$$

Then for $r_2+\epsilon \le r \le r_3-\epsilon$, $\epsilon>0$, $Q^2(r) \to +\infty$ as $g \to +\infty$ and

$$\psi \approx \cos[Q(r_0)(r-r_2) + \mathrm{const}]$$

is infinitely oscillatory, thus corresponding to resonances or Regge trajectories whose radial quantum number n is

TABLE I. $I=\frac{3}{2}$, $J=l+\frac{1}{2}$, odd l, odd J signature, positive parity.

J	$\frac{3}{2}^+$	$\frac{7}{2}^+$	$\frac{11}{2}^+$	$\frac{15}{2}^+$	$19/2^+$
m	1.236	1.95	2 42	2.85	3.23
m^2	1.53	3.83	5.86	8.12	10.43
Γ_{el}	0.125	0.084	0.034	0.012	0.002
Γ_{tot}	0.125	0.210	0.31	0.4	0.44
Γ_{el}/Γ_{tot}	1	0.4	0.11	0.03	0.005
J	$\frac{3}{2}^+$	$\frac{7}{2}^+$	$\frac{11}{2}^+$	$\frac{15}{2}^+$	
m	1.69				
m^2	2.86	~4.86			
Γ_{el}	0.028				
Γ_{tot}	0.28				
Γ_{el}/Γ_{tot}	0.1				
J	$\frac{3}{2}^+$	$\frac{7}{2}^+$	$\frac{11}{2}^+$	$\frac{15}{2}^+$	
m					
m^2	~4.7				
Γ_{el}	(dip,η)				
Γ_{tot}					
Γ_{el}/Γ_{tot}					

tending to infinity. Since the leading trajectories are of interest to us, we take

$$\lambda^2/g \to \phi(r_0) \quad \text{as} \quad g \to \infty , \tag{2.8}$$

so that the oscillations of ψ are now finite in number.

In order to obtain an expression for $\mathrm{Re}\alpha_n$, n finite, we utilize the eigenvalue equation arising in the JWKB formalism. The eigenvalue equation is, for $g \to \infty$,

$$\int_{r_2}^{r_3} dr\, Q(r) = (n+\tfrac{1}{2})\pi, \quad n=0, 1, 2, \cdots, <\infty . \tag{2.9}$$

It can be shown rigorously that the condition requiring the dominance of the "outgoing-wave" part of the regular solution over the "incoming-wave" part in the region between r_3 and r_4, in the limit $g \to \infty$, yields (2.9). Under the same limit, this condition is equivalent to the Regge-pole condition. This, of course, means that $\mathrm{Im}\alpha_n \to 0$ as $g \to \infty$. Hence we set $\lambda = \mathrm{Re}\alpha_n$ in (2.9). Now because of the condition (2.8)

$$r_2 \to r_0 - 0 \quad \text{and} \quad r_3 \to r_0 + 0 ,$$

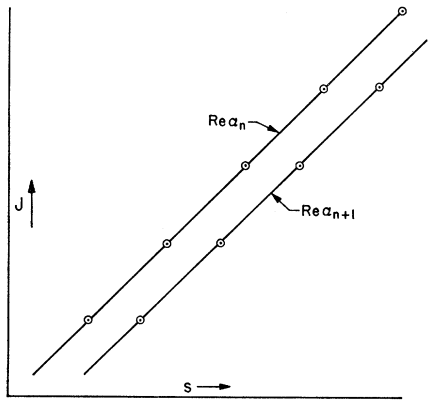

FIG. 3. Chew-Frautschi plot for radial-quantum-number trajectories. For simplicity, trajectory forms $\mathrm{Re}\alpha_n = \sqrt{2}n + a + s$ have been chosen.

the behavior of $\phi(r)$ near its maximum r_0 is relevant. We thus approximate $\phi(r)$ by

$$\phi(r) = \phi(r_0) - \frac{1}{2}\left|\frac{d^2\phi(r_0)}{dr^2}\right|(r-r_0)^2 ,$$

which yields

$$Q^2(r) = -ga_1 + ga_2 1/r - (\lambda^2/r^2)a_3 . \tag{2.10}$$

In (2.10) we have

$$a_1 = \frac{1}{2}\left|\frac{d^2\phi}{dr^2}\right|_{r_0} \xrightarrow[q^2/g\to 0]{} \tfrac{1}{2}k\left(\frac{\eta+1}{k}\right)^{\eta} e^{-(\eta+1)} ,$$

$$a_2 = r_0\left|\frac{d^2\phi}{dr^2}\right|_{r_0} \xrightarrow[q^2/g\to 0]{} k\left(\frac{\eta+1}{k}\right)^{\eta+1} e^{-(\eta+1)} , \tag{2.11}$$

$$a_3 = \frac{r_0^2}{2\phi(r_0)}\left|\frac{d^2\phi}{dr^2}\right|_{r_0} \xrightarrow[q^2/g\to 0]{} \tfrac{1}{2}(\eta+1) ,$$

where, in writing a_3, condition (2.8) has been used; the results in (2.7) have been used in writing the limiting forms as $q^2/g \to 0$. With the use of $Q^2(r)$ given by (2.10) in (2.9) the problem reduces mathematically to the familiar hydrogen-atom problem. The resulting expression is

$$\mathrm{Re}\alpha_n = -\frac{n+\frac{1}{2}}{(a_3)^{1/2}} + \tfrac{1}{2}a_2\left(\frac{g}{a_1 a_3}\right)^{1/2} ,$$

and since empirical evidence suggests that $q^2/g \to 0$, we utilize the limiting forms in (2.11) and obtain

$$\mathrm{Re}\alpha_n = -\left(\frac{2}{\eta+1}\right)^{1/2} n + a + \left(\frac{g}{2ek}\right)^{1/2}(\eta+1)\left(\frac{\eta+1}{ek}\right)^{\eta/2} , \tag{2.12}$$

where

$$n=0, 1, 2, 3, \cdots, <\infty , \quad -1<\eta<\infty ,$$

and a is a constant which has been introduced but is not essential.

For a given η, the pattern on the Chew-Frautschi plot is clear. Let $s_n(J)$ be the value of s for which

$$\mathrm{Re}\alpha_n = -\left(\frac{2}{\eta+1}\right)^{1/2} n + a + (\eta+1)\left(\frac{\eta+1}{ek}\right)^{\eta/2}\left(\frac{g(s)}{2ek}\right)^{1/2} = J ,$$

where J is physical spin. Then, on using the monotonic increase of g with respect to s, we conclude from

$$[g(s_{n+1}(J))]^{1/2} - [g(s_n(J'))]^{1/2} = \left[\left(\frac{2}{\eta+1}\right)^{1/2} - (J'-J)\right]\frac{(2ek)^{1/2}}{\eta+1}\left(\frac{ek}{\eta+1}\right)^{\eta/2}$$

that

if $J'=J$, then $s_{n+1}(J)>s_n(J)$,

if $J'>J$ and $J'-J<[2/(\eta+1)]^{1/2}$, then $s_{n+1}(J)>s_n(J')$,

if $J'>J$ and $J'-J>[2/(\eta+1)]^{1/2}$, then $s_{n+1}(J)<s_n(J')$,

if $J'>J$ but $J'-J=[2/(\eta+1)]^{1/2}$, then $s_{n+1}(J)=s_n(J')$.

We can see that for large η, $s_{n+1}(J)$ approaches $s_n(J)$ from above and that trajectories with finite n squeeze together. Simultaneously, the slopes of these trajectories also increase. For $\eta=-1+\epsilon$, ϵ small but positive, the trajectories are widely separated, $s_{n+1}(J)\gg s_n(J)$, and they tend to become almost flat trajectories. We may remark here that $\eta>0$ may occur if there is a cancellation between the exchanged trajectories resulting in a decrease of the singular nature of the equivalent potential at $r=0$. For our purpose, we consider $\eta=0$ only [Eq. (2.3)], in which case (see Fig. 3)

$$s_n(J+2)>s_{n+1}(J)>s_n(J). \tag{2.13}$$

The general expression for Imα is well known and is given by

$$\mathrm{Im}\alpha_n=\frac{1}{2\,\mathrm{Re}\alpha_n+1}\frac{1}{2i}\left[\psi^*\frac{d\psi}{dr}-\psi\frac{d\psi^*}{dr}\right]_{r=\infty}\Big/\int_0^\infty dr\frac{|\psi|^2}{r^2},$$

where

$$\psi\equiv\psi(\alpha_n,s,r).$$

Since it is known that Imα is small as a first approximation, we set $\alpha_n\equiv\mathrm{Re}\alpha_n$ in ψ. Utilizing the wave function from the JWKB formalism, we have

$$\mathrm{Im}\alpha_n=\frac{1}{2\,\mathrm{Re}\alpha_n+1}\exp\left[-2\int_{r_3}^{r_4}dr|Q(r)|\right]\Big/\int_0^\infty dr\frac{|\psi|^2}{r^2}$$

$$\equiv[s_n(J)]^{1/2}\frac{d\alpha_R}{ds}\bigg|_{s_n(J)}\Gamma(s_n(J)). \tag{2.14a}$$

The exponential function represents the probability of tunneling through the centrifugal barrier. We may thus replace it by a more accurate expression and write

$$[s_n(J)]^{1/2}\frac{d\alpha_R}{ds}\bigg|_{s_n(J)}\Gamma(s_n(J))\equiv\mathrm{Im}\alpha_n$$

$$=\left\{(2\,\mathrm{Re}\alpha_n+1)\left[1+\exp\left(2\int_{r_3}^{r_4}dr|Q(r)|\right)\right]\times\int_0^\infty dr\frac{|\psi|^2}{r^2}\right\}^{-1}. \tag{2.14b}$$

Furthermore, we can easily arrive at the following estimates:

$$\int_0^\infty dr\frac{|\psi|^2}{r^2}=O(1/\sqrt{g}),$$

$$\exp\left\{-2\int_{r_3}^{r_4}dr|Q(r)|\right\}<\exp[-(\sqrt{g})(r_4-r_3-2\epsilon)O(1)],$$

with

$$r_4\approx(\mathrm{Re}\alpha_n)/q\to\infty;$$

hence $\Gamma\sim(1/\sqrt{s})e^{-g/q}$, $g\sim s^2$ as suggested empirically. It would be more appropriate to view the above results as showing that the elastic half-width, or the residue of the Regge pole, is a rapidly decreasing function as $s\to+\infty$. The rapid decrease of the half-width is due to the increasing region in which the centrifugal barrier is present, as well as increase in its height as $\mathrm{Re}\alpha_n\to\infty$ with s.

For the leading trajectories, the radial quantum number is finite and negligible in the exponential entering (2.14); thus we expect their elastic half-widths to be of the same order as that for the leading trajectory for the same energy regions.

TABLE II. $I=\frac{1}{2}$, $J=l-\frac{1}{2}$, odd l, even J signature, positive parity.

J	$\frac{1}{2}^+$	$\frac{5}{2}^+$	$\frac{9}{2}^+$
m	0.94	1.69	
m^2	0.88	2.86	∼4.86
Γ_{el}		0.076	
Γ_{tot}		0.125	
Γ_{el}/Γ_{tot}		0.6	
J	$\frac{1}{2}^+$	$\frac{5}{2}^+$	
m	1.46		
m^2	2.13	∼4.13	
Γ_{el}	0.143		
Γ_{tot}	0.26		
Γ_{el}/Γ_{tot}	0.55		
J	$\frac{1}{2}^+$	$\frac{5}{2}^+$	
m	1.785		
m^2	3.19		
Γ_{el}	0.136		
Γ_{tot}	0.405		
Γ_{el}/Γ_{tot}	0.34		

III. COMPARISON WITH BARYON SPECTRUM

In this section[5] we examine the nonstrange baryon spectrum[6] in order to verify the existence of higher-radial-quantum-number trajectories satisfying

$$s_n(J+2)>s_{n+1}(J)>s_n(J), \tag{3.1}$$

where $s_n(J)$ is the mass squared of a particle with spin

[5] The masses are in units of GeV.

[6] A. Donnachie, in *Proceedings of the Fourteenth International Conference on High-Energy Physics, Vienna, 1968* (CERN, Geneva, 1968), p. 139; C. Lovelace, in *Proceedings of International Conference on Elementary Particles, Heidelberg, 1967*, edited by H. Filthuth (North-Holland Publishing Co., Amsterdam, 1968), p. 79; V. Barger and D. Cline, Phys. Rev. **156**, 1522 (1967); Particle Data Group, Rev. Mod. Phys. **41**, 109 (1969).

TABLE III. $I=\frac{1}{2}$, $J=l-\frac{1}{2}$, l even ≥ 2, odd J signature, negative parity.

J	$\frac{3}{2}^-$	$\frac{7}{2}^-$	$\frac{11}{2}^-$	$\frac{15}{2}^-$
m	1.52	2.19	2.65	3.03
m^2	2.295	4.8	7.0	9.2
Γ_{el}	0.058	0.105	0.027	0.0024
Γ_{tot}	0.115	0.30	0.36	0.4
Γ_{el}/Γ_{tot}	0.5	0.35	0.075	0.006
J	$\frac{3}{2}^-$	$\frac{7}{2}^-$		
m	1.7			
m^2	2.89	$\sim$4.89		
Γ_{el}	0.075	(decreasing η)		
Γ_{tot}	0.3			
Γ_{el}/Γ_{tot}	0.25			
J	$\frac{3}{2}^-$			
m	1.98			
m^2	3.92			
Γ_{el}				
Γ_{tot}				
Γ_{el}/Γ_{tot}				

TABLE V. $I=\frac{3}{2}$, $J=l-\frac{1}{2}$, l odd ≥ 3, even J signature, positive parity.

J	$\frac{5}{2}^+$	$\frac{9}{2}^+$
m	1.91	
m^2	3.61	$\sim$5.61
J	$\frac{5}{2}^+$	
m		
m^2	$\sim$5.0	

J and the radial quantum number n. For the degree of credulity associated with each particle, see the quoted references.[6] We may state here that the leading trajectories displayed in Tables I–III have more than one well-established resonance. In the tabulation "dip η" means that the elasticity decreases here in the CERN set of phase shifts, but no resonance has been claimed. The symbol $\sim$ refers to the prediction of a resonance.

To begin with, let us consider the nucleon and Δ set of trajectories (Tables I and II). Accompanying the leading nucleon and Δ trajectories, we observe the first manifestations of deeper-lying trajectories having the same quantum numbers. The masses of the first manifestations satisfy inequality (3.1) very well. With the expected Regge-trajectory slope, ≈ 1 GeV^{-2}, it is certain that the higher recurrences also satisfy (3.1). Clearly, then, it is reasonable to interpret these deeper-lying trajectories as the higher-radial-quantum-number trajectories associated with the leading nucleon and Δ trajectories.

We recall that we have considered the nucleon and Δ trajectories as reciprocally bootstrapping each other in the πN channel. As a consequence, higher-radial-quantum-number trajectories were predicted. It is thus interesting to note that $N(1.460)$, the Roper resonance, is an outcome of the reciprocal bootstrap of the nucleon and Δ trajectories.

The above case also shows that a single channel (πN) is sufficient to explain the nucleon and Δ set of trajectories. Such a simple circumstance need not occur always. Thus, for example, we could have two dynamically significant channels weakly coupled to each other. Each channel would then yield its set of trajectories satisfying (3.1). In this event, the empirical spectrum would not display the pattern (3.1) as readily as it has in the case of the nucleon and Δ trajectories.

In Table III, the D_{13} trajectories again satisfy (3.1), thus indicating that here also only one channel is active. We will now turn to some of the other resonances that have been seen. One $P_{31}(1.930)$, $m^2=3.63$ and one $F_{35}(1.910)$, $m^2=3.61$ are observed; the only reasonable choice is to attribute different trajectories to the two particles (Tables IV and V). From our point of view we have to assign different two-particle channels to account for their existence. The particle channel associated with the trajectory on which $F_{35}(1.910)$ lies is such that the point having P_{31} quantum numbers in the πN channel is a nonsense point for it. Next consider $S_{31}(1.64)$, $m^2=2.69$ and $D_{35}(1.95)$, $m^2=3.8$; the former has been ranked "good" and the latter "poor."[6] If the particles are assigned to the same trajectory, the resultant slope is ≈ 1.8 GeV^{-2}, which would require a G_{39} with $m^2=4.9$. The CERN set of phase shifts[6] does not show a dip in the elasticity for G_{39} until 4.92. Furthermore, the first higher radial quantum number S_{31} would have $m^2\approx 3.2$; no resonant behavior is observed here. Hence it is preferable to retain an ≈ 1 GeV^{-2} slope and consider two separate trajectories. Thus the next recurrence, D_{35}, of the $S_{31}(1.64)$ trajectory is expected to occur at $s\approx 4.69$, and the next higher radial quantum number S_{31} at $s\approx 4.1$ (Table VI). As regards the $D_{35}(1.95)$ trajectory, if it survives, it will be due to a single channel for which S_{31} is a nonsense point. The higher-radial-quantum-number trajectories associated with $D_{35}(1.95)$ trajectory, from our point of view, will have their S_{31} points also as nonsense points. Finally, we have $D_{33}(1.69)$, $m^2=2.79$, which obviously implies G_{37}, $m^2=4.79$ on the leading trajectory, and a second D_{33}, $m^2\approx 4.2$ (Table VII).

TABLE IV. $I=\frac{3}{2}$, $J=l-\frac{1}{2}$, l odd, even J signature, positive parity.

J	$\frac{1}{2}^+$	$\frac{5}{2}^+$
m	1.93	
m^2	3.63	$\sim$5.63
J	$\frac{1}{2}^+$	
m		
m^2	$\sim$5.0	

TABLE VI. $I=\frac{3}{2}$, $J=l+\frac{1}{2}$, l even, even J signature, negative parity.

J	$\frac{1}{2}^-$	$\frac{5}{2}^-$
m	1.64	
m^2	2.69	$\sim$4.69
J	$\frac{1}{2}^-$	
m		
m^2	$\sim$4.1	

TABLE VII. $I=\frac{3}{2}$, $J=l-\frac{1}{2}$, l even, odd J signature, negative parity.

J	$\frac{3}{2}^-$	$\frac{7}{2}^-$
m	1.69	
m^2	2.79	~4.79
J	$\frac{3}{2}^-$	
m		
m^2	~4.2	

Turning to the remaining isospin-$\frac{1}{2}$ particles, we will consider the following only: $S_{11}(1.525)$, $m^2=2.33$; $D_{15}(1.675)$, $m^2=2.81$; and $S_{11}(1.715)$, $m^2=2.94$. All these particles are ranked "established."[6] We are again faced with two possibilities. The first (Tables VIII and IX) is to consider $S_{11}(1.525)$, $m^2=2.33$ and $D_{15}(1.675)$, $m^2=2.82$ as occurring on different trajectories, S_{11} being a nonsense point for the $D_{15}(1.675)$ trajectory and its associates. The next recurrence of the $S_{11}(1.525)$ trajectory, D_{15}, is expected at $s\approx 4.33$. Clearly, then, $S_{11}(1.71)$, $m^2=2.92$ is the first manifestation of the first radial-quantum-number trajectory associated with the $S_{11}(1.525)$ trajectory. The second possibility (Table X) is to consider $S_{11}(1.525)$ and $D_{15}(1.675)$ to be lying on the same trajectory. This choice requires a large variation of the slope of the trajectory. This variation has to be of a local character since no resonance is observed in the G_{19} amplitude until $s\approx 4.9$. In previous constructions, large departures from unit slope have been rejected. But in the present instance we retain this possibility in order to point out a mechanism which could cause such variations. This mechanism arises from the effect of other channels and is discussed in the next section. Of course, $S_{11}(1.71)$ is still considered the first radial excitation of $S_{11}(1.525)$.

Before concluding this section, it may be pointed out that the difference in m^2 for two resonances having the same quantum numbers is $\sqrt{2}$ as given by Eq. (2.12) ($\eta=0$, and $g/2ek=s^2$ as suggested empirically). This difference in m^2 is fairly well satisfied in Tables I–III, and has been used in the predictions listed in the remaining tables. We would, however, stress that inequality (3.1) is the prediction for the pattern of resonances, since, although the multichannel effects are small as seen from Tables I–III, their effect would certainly shift the masses from that expected from Eq. (2.12) for the Yukawa potential.

An analogous comparison may be carried out for the boson spectrum. However, such an exercise would be little different from that carried out for the quark model.[7]

TABLE VIII. $I=\frac{1}{2}$, $J=l+\frac{1}{2}$, l even, even J signature, negative parity.

J	$\frac{1}{2}^-$	$\frac{5}{2}^-$
m	1.525	
m^2	2.33	~4.33
J	$\frac{1}{2}^-$	
m	1.715	
m^2	2.94	

TABLE IX. $I=\frac{1}{2}$, $J=l+\frac{1}{2}$, l even ≥ 2, even J signature, negative parity.

J	$\frac{5}{2}^-$	$\frac{9}{2}^-$
m	1.675	
m^2	2.81	~4.81
J	$\frac{5}{2}^-$	
m		
m^2	~4.22	

IV. BEHAVIOR OF Imα

In this section we consider the multichannel nature of the problem and suppose that a number N of two-particle channels is relevant in a given energy region of interest. We thus consider an N-channel differential equation of the form

$$\frac{d^2}{dr^2}\psi+\mathbf{v}\psi=0, \quad \mathbf{v}=\mathbf{q}^2+\mathbf{V}-(\mathfrak{L}^2-\tfrac{1}{4})/r^2, \qquad (4.1)$$

where ψ and $\mathbf{V}$ are $N\times N$ matrices, whereas $\mathbf{q}^2$ and $\mathfrak{L}^2$ are diagonal $N\times N$ matrices. For the ith two-particle channel, we have

$$q_i^2=[s-(m_{1i}+m_{2i})^2][s-(m_{1i}-m_{2i})^2]/4s,$$

and $l_i=\lambda_i-\frac{1}{2}$ represents the ith-channel orbital angular momentum which, when combined with the channel spin, gives rise to the total angular momentum J of the whole system.

In order to simplify the problem, we approximate the differential equation (4.1) by another for which

$$\begin{aligned} v_{ij}=&-k_{\mathrm{I}i}^2\delta_{ij}\theta(r)\theta(r_2-r) && \text{(region I)}\\ &+\sum_p (U^\dagger)_{ip}k_{\mathrm{II}p}^2U_{pj}\theta(r-r_2)\theta(r_3-r) && \text{(region II)}\\ &-k_{\mathrm{III}i}^2\delta_{ij}\theta(r-r_3)\theta(r_{4i}-r) && \text{(region III)}\\ &+q_i^2\delta_{ij}\theta(r-r_{4i}) && \text{(region IV)},\\ &\theta(r)=1 \text{ if } r>0 \\ &\quad=0 \text{ if } r<0. && (4.2)\end{aligned}$$

TABLE X. Alternative to Tables VIII and IX; see Fig. 4. $I=\frac{1}{2}$, $J=l+\frac{1}{2}$, l even, even J signature, negative parity.

J	$\frac{1}{2}^-$	$\frac{5}{2}^-$
m	1.525	1.675
m^2	2.33	2.81
J	$\frac{1}{2}^-$	
m	1.715	
m^2	2.94	

[7] H. Harari, in *Proceedings of the Fourteenth International Conference on High-Energy Physics, Vienna, 1968* (CERN, Geneva, 1968), p. 195.

The S matrix for (4.2) is given by[8]

$$(E_{\mathrm{IV}}^{-})^{-1}S(E_{\mathrm{IV}}^{-})^{-1}=-S_{\mathrm{IV}}, \tag{4.3}$$

$$S_{\mathrm{IV}}=(K_{\mathrm{IV}}-i)(K_{\mathrm{IV}}+i)^{-1}, \tag{4.4}$$

where

$$E_{\mathrm{IV}ij}^{-}=e^{-iq_ir_{4i}}\delta_{ij}. \tag{4.5}$$

Matrix S denotes the ratio of the coefficient matrices of the $e^{+iqr}/\sqrt{q}$ and $e^{-iqr}/\sqrt{q}$ matrices. For the K_{IV} matrix, we have the expressions

$$\begin{aligned}K_{\mathrm{IV}}&=q^{1/2}R_{\mathrm{IV}}q^{1/2},\quad R_{\mathrm{IV}}{}^{\dagger}=R_{\mathrm{IV}}\\&=qk_{\mathrm{III}}{}^{-1}+(2qk_{\mathrm{III}}{}^{-1}E_{\mathrm{III}}{}^{-2})^{1/2}(S_{\mathrm{III}}-E_{\mathrm{III}}{}^{-2})^{-1}\\&\qquad\times(2qk_{\mathrm{III}}{}^{-1}E_{\mathrm{III}}{}^{-2})^{1/2},\end{aligned} \tag{4.6}$$

where

$$E_{\mathrm{III}ij}{}^{-2}=\exp[-2k_{\mathrm{III}i}(r_{4i}-r_3)]\delta_{ij} \tag{4.7}$$

and

$$S_{\mathrm{III}}=(K_{\mathrm{III}}+1)(K_{\mathrm{III}}-1)^{-1}, \tag{4.8}$$

with

$$K_{\mathrm{III}}=k_{\mathrm{III}}{}^{1/2}U^{\dagger}R_{\mathrm{II}}Uk_{\mathrm{III}}{}^{1/2}. \tag{4.9}$$

The matrix $U^{\dagger}R_{\mathrm{II}}U$ contains information regarding region II, where the effect of the potential matrix is dominant. Supposing that k_{1i} is very large for every i, we have

$$R_{\mathrm{II}ij}=\frac{\sin k_{\mathrm{II}i}(r_3-r_2)}{k_{\mathrm{II}i}\cos k_{\mathrm{II}i}(r_3-r_2)}\delta_{ij}.$$

Following the usual procedure, the resonance condition is

$$\det K_{\mathrm{IV}}{}^{-1}=0,$$

which reduces to

$$\det(S_{\mathrm{III}}-E_{\mathrm{III}}{}^{-2})=0,$$

as can be easily seen from (4.6). Let Λ and $\mathfrak{L}$ be unitary matrices which diagonalize K_{IV} and $S_{\mathrm{III}}-E_{\mathrm{III}}{}^{-2}$, respectively. Further, let the resonant eigenchannel of $S_{\mathrm{III}}-E_{\mathrm{III}}{}^{-2}$ be indexed by 1, and resonant at $\sqrt{s}=w=m$ with total angular momentum J. The expression for partial half-widths is given by

$$\Gamma_{i1}{}^{1/2}=\left(\frac{q_iE_{\mathrm{III}i}{}^{-2}}{K_{\mathrm{III}i}}\gamma_1\right)^{1/2}\mathfrak{L}_{i1}=\Lambda_{i1}\Gamma_1{}^{1/2},\quad w=m \tag{4.10}$$

where $-\gamma_1$ is the residue of $[\mathfrak{L}^{\dagger}(S_{\mathrm{III}}-E_{\mathrm{III}}{}^{-2})^{-1}\mathfrak{L}]_{11}$ and Γ_1 the total width of the resonance.

The discussion in Sec. III has shown that the expected pattern of resonances on the basis of single-channel dynamics is well satisfied and that departures due to multichannel effects are not large. We thus assume that the off-diagonal elements of the potential matrix, or v_{ij} in region II, are small. Or, in a more direct fashion, it is assumed that the off-diagonal elements of K_{III} are small. This latter assumption will be utilized from now on.

Let the $i=1$ particle channel be principally responsible for the resonances in the eigenchannel 1. The resonances we consider are those which lie on the same trajectory $J=\mathrm{Re}\alpha=a+m^2$; furthermore, m will be treated as a continuous parameter. Now, $\mathfrak{L}_{i1}$ represents the projection of the ith-particle-channel vector onto the resonant eigenvector in the interior region II, which is responsible for the formation of the resonance (or the Regge trajectory). Our assumption thus implies that $|\mathfrak{L}_{i1}|^2$, $i=1$, will be dominant over $|\mathfrak{L}_{i1}|^2$, $i\neq 1$. The analysis in Sec. II suggests that

$$\frac{(k_{\mathrm{III}})_1}{(k_{\mathrm{II}})_1}\approx\frac{\lambda_1}{\sqrt{g}}\approx\frac{\mathrm{Re}\alpha}{m^2}=\text{const},\quad q_1/(k_{\mathrm{III}})_1\to 0$$

where $\sqrt{g}\approx m^2$, as empirically suggested, has been utilized. From (4.10) we see that the partial width Γ_{11} will tend to zero as $m\to\infty$. Now if the total width Γ_1 does not decrease as rapidly, or does not decrease at all, then Λ_{i1}, $i=1$, will be very small. This of course shows that the smallness of Γ_{i1}/Γ_1, a highly inelastic resonance in the ith particle channel, does not necessarily imply that this particle channel is insignificant in the formation of the resonance.

In the expression for Γ_{11}, let us set $\mathfrak{L}_{11}=1$ and compare with (2.14a); the comparison is obvious, and we conclude that $\gamma_1=O(1)$. Under our assumption, we expect $\gamma_1=O(1)$ even when $\mathfrak{L}_{11}\lesssim 1$. Further, since

$$|\mathfrak{L}_{11}|^2=1-\sum_{i\neq 1}|\mathfrak{L}_{i1}|^2, \tag{4.11}$$

and $|\mathfrak{L}_{11}|^2$ is considered dominant, the variation of $\mathfrak{L}_{i1}$, $i\neq 1$, with m along the Regge trajectory will not be drastic. From (4.10) we see that the main contribution to the total half-width arises from particle channels with low orbital angular momenta; that is, from those channels with high channel spin. The threshold of such channels will of course be in the neighborhood of m, so that $q_i/k_{\mathrm{III}i}\approx r_{4i}=O(1)$ along with

$$\exp[-2K_{\mathrm{III}i}(r_{4i}-r_3)].$$

Since we have assumed that channels with low channel spin are primarily responsible for generating the Regge trajectories, the channels with large channel spin do not have a dynamically significant role. Thus, choosing the simplest possiblity, we may attribute roughly equal weight, $|\mathfrak{L}_{i1}|^2$, to them consistent with the dominance of $|\mathfrak{L}_{11}|^2$. The behavior of the total half-width with m thus will essentially depend upon the number of channels with low orbital angular momenta into which the resonance (m, $J=a+m^2$) will decay. We turn our attention to this aspect.

To begin with, we count the number of channels which result on taking pairs of particles lying on two

[8] We have treated the problem like an S-wave one, with the the centrifugal force treated like a repulsive potential. This is, of course, not correct if we were interested in studying the phase shifts. However, the present expressions provide a simpler framework for the discussion in this section. None of the physical ideas and conclusions is altered if we were to adopt the more accurate expressions.

trajectories, one from each. Let the two trajectories be

$$J_1=(j_1-m_{01}^2)+m_1^2 \quad \text{and} \quad J_2=(j_2-m_{02}^2)+m_2^2,$$

where m_{01} and m_{02} are the lowest particle masses on each trajectory. Let J and m be the resonance of interest lying on the trajectory

$$J=(j-m_0^2)+m^2,$$

and let the orbital angular momenta of interest range from zero to L. The channel spins of interest are thus

$$J+L,\quad J+L-1,\quad J+L-2,\cdots,\quad J-L>0.$$

Particles with masses m_1 and m_2 for which

$$J_1+J_2<J-L$$

is true are clearly not relevant. Similarly, those m_1 and m_2 for which

$$J_1-J_2>J+L$$

or

$$J_2-J_1>J+L$$

is true are again not of interest. Thus those (m_1,m_2) for which at least one of their channel spins lies in the range $J-L$ to $J+L$ are contained in the closed domain bounded by the curves C_1, C_2, and C_3, and with $m_1\geq m_{01}$ and $m_2\geq m_{02}$ (Fig. 4). The curves C_1, C_2, and C_3 are defined by

$$\begin{aligned}
&C_1:\quad m_1^2+m_2^2=(J-L-j_1-j_2+m_{01}^2+m_{02}^2)=R_1^2,\\
&C_2:\quad m_1^2-m_2^2=(J+L-j_1+j_2+m_{01}^2-m_{02}^2)=R_2^2,\\
&\qquad\qquad J_1>J_2 \qquad (4.12)\\
&C_3:\quad m_2^2-m_1^2=(J+L-j_2+j_1+m_{02}^2-m_{01}^2)=R_3^2,\\
&\qquad\qquad J_2>J_1.
\end{aligned}$$

Finally, we have to take account of the condition

$$\begin{aligned}
&m_1+m_2<m=(J-j+m_0)^{1/2},\\
&C_4:\quad m_1+m_2=(J-j+m_0)^{1/2}.
\end{aligned}\qquad (4.13)$$

For large J, the allowed domain is shown shaded in Fig. 4. Clearly we must require that the following conditions are satisfied:

$$\text{(i)}\quad m^2-R_1^2>0,$$
$$\text{(ii)}\quad m_{1C}-m_{01}>0,$$

where m_{1C} is the m_1 common to C_1 and C_4. Condition (i) requires

$$\text{(ia)}\quad L+j_1+j_2-j+m_0^2>m_{01}^2+m_{02}^2,$$

and for finite L and m_0 (j_1, j_2, and j are always finite), m_{01} and m_{02} will be bounded, so that $m^2-R_1^2$ is bounded when L is finite. This of course means that for finite L,

$$m-R_1=\frac{m^2-R_1^2}{m+R_1}\sim\frac{1}{\sqrt{J}}\to+0.$$

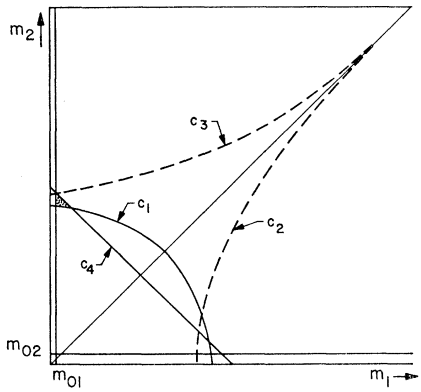

FIG. 4. (m_1,m_2) plane formed by mass points lying on the Regge trajectory $J_1=a_1+m_1^2$ and mass points on the Regge trajectory $J_2=a_2+m_2^2$. The channels into which a particle with mass m and spin $J=a+m^2$ is allowed to decay lie in the shaded region.

Condition (ii) requires

$$\text{(iia)}\quad \tfrac{1}{2}m\{1-[1-2(m^2-R_1^2)/m^2]^{1/2}\}>m_{10},$$

which, for finite L, reads

$$\text{(iib)}\quad (m^2-R_1^2)/2m_{10}>m.$$

Condition (ii) for finite L thus clearly shows that if $m_{10}\neq 0$, the decay of the resonance (J,m) into two particle channels with finite orbital angular momenta, for sufficiently large m, is kinematically not possible. Of course, if $m_{10}=0$, then no such restriction follows.

Let us continue with the requirement L finite, and we suppose that we have chosen some fixed L. Now the trajectory which comes closest to satisfying the condition $m_{10}=0$ is the pion trajectory. Thus for fairly large m satisfying (iib), the favored two-particle decays are those in which one of the particles is a pion and the orbital angular momenta are finite. The number of available two-particle channels then clearly is the nearest integer less than $\frac{1}{2}(m^2-R_1^2)$ if $\Delta J=2$ rule or $m^2-R_1^2$ if $\Delta J=1$ rule. Given L, j_1, j_2, j, m_{01}, and m_0, condition (ia) yields a restriction on m_{02}; that is, very-deep-lying trajectories are excluded. Consequently there are only a finite number of trajectories with which we can pair the pion trajectory. Hence for the trajectory $J=j-m_0^2+m^2$, the number of channels with $l\leq L$ increases as m increases, reaches a constant when all the trajectory pairs contribute, and remains constant as long as condition (iib) is well satisfied. If m_0^2 is increased, deeper-lying trajectories can pair with the pion trajectory, resulting in an increase in the number of decay channels.

Finally, we combine the discussion in the last paragraph with that given in the paragraph containing Eq. (4.11). The result then is that $\Gamma_{\text{tot } n=0}$ of the leading trajectory is expected to increase monotonically as m varies along the trajectory, flattening off beyond a certain point. For trajectories with higher radial quantum number (deeper-lying), $\Gamma_{\text{tot } n>0}$ will have the same be-

havior as for the leading one; however, we have $\Gamma_{\text{tot } n\neq 0} > \Gamma_{\text{tot } n=0}$. From the discussion on (2.14) we have that $\Gamma_{11,n\neq 0} \approx \Gamma_{11,n=0}$ for the same mass region. Hence, resonances with radial quantum number n will be more inelastic than those with $n-1$ and lying in the same mass region. One may compare these results with the empirical behavior in Tables I and III.

It should be stressed that the foregoing comparison with data is under condition (iib). With $m_{01}=$ pion mass and $L=4$, we see that for the leading N, Δ, and $\{I=\frac{1}{2}, J^P=(l-\frac{1}{2})^-, l=2, 4, 6, \cdots\}$ trajectories the range of allowed m is ample for the comparison to be meaningful. However, for $m\to\infty$, two-particle decay channels with finite orbital angular momenta are no longer kinematically possible for trajectories varying linearly with $m^2\equiv s$.

The circumstance stated in the last paragraph, $m_{1C}\to 0$ as $m\to\infty$, is intimately related with $m-R_1\to 0$ as $m\to\infty$. Retaining the assumption that L is finite, we consider other trajectory functions whose form is taken to be valid for all trajectories. It can be easily seen that $m-R_1\to 0$ for trajectory functions with $\mathrm{Re}\alpha/\sqrt{s}\to\infty$ as $s\to+\infty$; $m-R_1 \not\to 0$ and remains bounded for trajectory functions with $\mathrm{Re}\alpha/\sqrt{s}=O(1)$ as $s\to+\infty$; and $m-R_1\to+\infty$ for trajectory functions with $\mathrm{Re}\alpha/\sqrt{s}\to 0$, $\mathrm{Re}\alpha\to+\infty$ as $s\to+\infty$. If $\alpha(s)$ does not have an essential singularity at $s=\infty$, then the second and third cases are not of interest; as $s\to-\infty$ in the second case, $\alpha\to\pm i\infty$, and in the third case $\mathrm{Re}\alpha\to+\infty$ as $s\to-\infty$. Thus we are left with the conclusion that for trajectory functions for which $\mathrm{Re}\alpha/\sqrt{s}\to+\infty$ (physically interesting trajectories, $\alpha\to-\infty$ as $s\to-\infty$, are contained in this class), $m_{1C}\to 0$, so that two-particle decay channels with finite orbital angular momenta are no longer kinematically possible for resonances with sufficiently high mass.

One may be led to suspect that $\Gamma_{\text{tot}}\to 0$ as $\sqrt{s}=m\to+\infty$; however, we still have the possibility that $L=L(m)\to+\infty$ as $m\to+\infty$. Assuming that trajectories vary linearly with m^2, one can estimate the number of available decay channels for various forms for $L(m)$. The number will now depend also on the number of deep-lying trajectories. Finally, the behavior of Γ_{tot} will require a more detailed knowledge of $\mathfrak{L}_{i1}$ [Eq. (4.10)] as a function of m. Especially when $r_4\simeq L/q \approx r_3\cong 1$ GeV, a more detailed knowledge of the potential would be necessary. At the present stage, therefore, we cannot even draw firm qualitative conclusions regarding the behavior of Γ_{tot}, or $\mathrm{Im}\alpha$, as $m^2=s\to+\infty$.

Multichannel Effects on Reα

Let us denote the trajectory function generated by a single channel, discussed in Sec. II, by $\alpha_0(s)$. Since empirically $\alpha_0(s)\cong a_0+b_0 s$, we may assume that $\alpha_0(s)$ is an entire function with respect to s. We are now interested in the shift of the trajectory function when $\mathrm{Im}\alpha$ is "switched on"; that is, the decay widths of the resonances are taken into account. Thereby we also take into account the multichannel effects on the resonance positions. To carry out our discussion, we assume that the observed trajectory function $\alpha(s)$ satisfies a subtracted dispersion relation, and that $\Gamma_{\text{tot}}\not\to\infty$ as well as $d\,(\mathrm{Re}\alpha)/ds \not\to \infty$ with $s\to+\infty$ as is suggested empirically. Taking this into account, it suffices to consider a once-subtracted dispersion relation; hence,

$$\mathrm{Re}\alpha(s)=[\mathrm{Re}\alpha(s_0)-\alpha_0(s_0)]+\alpha_0(s) +[\Delta(s)-\Delta(s_0)], \quad (4.14)$$

with

$$\Delta(s)=\frac{s}{\pi}P\int_{s_1}^{\infty}\frac{ds'}{\sqrt{s'}}\frac{\gamma(s')}{s'-s} \quad (4.15)$$

and

$$\gamma(s')=\frac{\mathrm{Im}\alpha(s')}{\sqrt{s'}}\equiv\frac{d\,\mathrm{Re}\alpha(s')}{ds'}\Gamma_{\text{tot}}(s'), \quad (4.16)$$

and where

$$\alpha_0(s)\cong a_0+b_0 s.$$

Now by assumption, $\alpha_0(s)\cong a_0+b_0 s$, $b_0\approx 1$, is generated by a single channel as suggested; thus the remaining terms in the right-hand side of Eq. (4.14) represent terms which include multichannel effects. The choice of the subtraction point may be taken in a region where multichannel effects are expected to be negilgible so that $\mathrm{Re}\alpha(s_0)\approx\alpha_0(s_0)$, in which case $\Delta(s)-\Delta(s_0)$ represents the shift. With the dynamical framework we have in mind, we consider $s_0\approx(m_\pi+m_N)^2$.

Let us first consider the leading trajectories in Tables I and III; in particular, we concentrate on the $D_{13}(1.52)$ trajectory. In this case, $d\,[\mathrm{Re}\alpha(s')]/ds'\approx 1$, so that $\gamma(s')\approx\Gamma_{\text{tot}}(s')$. Utilizing the empirical values for $\Gamma_{\text{tot}}(s')$, we represent the energy dependence of $\gamma(s')$ in a simple form by

$$\begin{aligned}\gamma(s')&=d(s'-s_1), && s_1\leqslant s'\leqslant s_3\\ &=0.4, && s_3\leqslant s'\end{aligned}$$
$$d=0.08,\quad s_1=1.2\approx(m_\pi+m_N)^2,\quad s_3=6.2 \quad (4.17)$$

and choose $s_0\equiv s_1$. The effect of the shift is displayed by the curves $\mathrm{Re}\alpha(s)$, empirical, and $\mathrm{Re}\alpha(s)-[\Delta(s)-\Delta(s_0)]$ given in Fig. 5. The maximum $\Delta(s)-\Delta(s_0)$ is roughly 0.8, occurring for $s\approx 5$, where $\gamma(s)$ is still increasing. This corresponds to roughly a 10% shift in mass. For large s, the shift $\Delta(s)-\Delta(s_0)\approx 0.25$, which corresponds to a negligible shift in mass for large m. The variation of $\Delta(s)$ is not rapid throughout.

In a fashion similar to the above, we may consider the leading $P_{33}(1.236)$ trajectory with

$$\begin{aligned}\gamma(s')&=d_1(s'-s_1), && s_1\leqslant s'\leqslant m_{N^*}{}^2\\ &=0.12+d_2(s'-m_{N^*}{}^2), && m_{N^*}{}^2\leqslant s'\leqslant s_3\\ &=0.45, && s'\geqslant s_3\end{aligned}$$
$$d_1=\tfrac{1}{3},\quad d_2=0.04,\quad s_1=(m_\pi+m_N)^2,$$
$$s_3=9.78,\quad m_{N^*}=1.236, \quad (4.18)$$

and $s_0 \equiv m_{N^*}{}^2$. Conclusions regarding the shift will be analogous to those from (4.17). Let us denote the variation of γ similar to those of (4.17) and (4.18) as "normal." From the discussion on Γ_{tot}, the "normal" behavior for γ is expected in general. Thus in the case of higher-radial-quantum-number trajectories also, the shift $\Delta(s)-\Delta(s_0)$ is expected to be analogous to that in Fig. 5 and of the same magnitude. Thus, as is evident, there would be little distortion of the pattern

$$s_n(J+2) > s_{n+1}(J) > s_n(J),$$

where n is the radial quantum number. Furthermore, the difference between $s_{n+1}(J)$ and $s_n(J)$ would be about $\sqrt{2}$, as noted towards the end of Sec. III. However, this difference is more sensitive to the details and hence the inequalities stated are more reliable.

The discussion regarding Γ_{tot} had been carried under the assumption that particle channel 1 was dominantly responsible for the formation of the trajectory in eigenchannel 1, so that $|\mathfrak{L}_{11}| \gg |\mathfrak{L}_{i1}|$, $i \neq 1$ [see (4.11)]. Furthermore, particle channels with $i \neq 1$ and low orbital angular momentum had been considered on an equal footing, so that $|\mathfrak{L}_{i1}| \approx |\mathfrak{L}_{j1}|$ for $i \neq 1$ and $j \neq 1$. It is possible, however, that one of these particle channels—the ith one, say—becomes dynamically significant in the formation of the trajectory for a local region of energy. The perturbative expression for the matrix U [Eq. (4.2)] suggests that this would occur if the off-diagonal element of the potential matrix V_{i1} suddenly became important, or if $V_{ii} \approx V_{11}$, or both, of course for a local energy region only. In such an event, $|\mathfrak{L}_{i1}|$ will be comparable to $|\mathfrak{L}_{11}|$, causing a sharp increase of Γ_{i1} [Eq. (4.10)] or Γ_{tot}, which would cause a similar variation in γ [Eq. (4.16)]. As can be seen from the dispersion relation satisfied by $\alpha(s)$, a sharp increase of γ reflects in a sudden increase of Reα.

In order to discuss numerically the phenomena stated in the last paragraph, we refer to Table X, where $S_{11}(1.525)$ and $D_{15}(1.675)$ have been assigned to the same trajectory, resulting in a rapid variation of Reα with s. It is evident from our previous discussion that a "normal" behavior for $\gamma(s)$ [see (4.17) or (4.18)] cannot account for the rapid variation of Reα found in this case. In fact, $\gamma(s)$ must have an almost step-function-like increase in the vicinity of the D_{15} resonance. Let us record the following two observations: First, it is seen that for $S_{11}(1.525)$ the $N\pi\pi$ decay mode is negligible, whereas for $D_{15}(1.675)$ almost 55% of the decay occurs through the $N\pi\pi$ mode[6]; secondly, we may observe that, taking the width of $D_{15}(1.68)$, $\Gamma_{\text{tot}} \approx 0.145$, into account, the energy level of this resonance overlaps the ρN threshold, $m_\rho + m_N \cong 1.694$, with $m_\rho \cong 0.755$. This suggests that the $N\pi\pi$ contribution to γ is negligible until we reach the ρN threshold, beyond which it very rapidly increases in an almost step-function-like manner. Thus we write

$$\gamma(s) = \gamma_0(s) + \gamma_\rho(s), \tag{4.19}$$

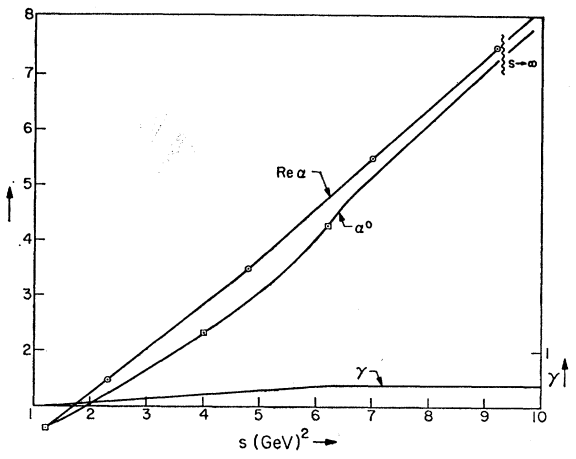

FIG. 5. Shift caused by Im$\alpha = (\sqrt{s})\gamma$ on the unperturbed leading D_{13} trajectory α_0 to give the observed leading D_{13} trajectory Reα. The continuous curve for α_0 is only to guide the eye.

where $\gamma_0(s)$ has a "normal" behavior and $\gamma_\rho(s)$ represents the contribution from the ρN channel. We also note that for sufficiently large s, because of the increasing centrifugal-barrier effects, $\gamma_\rho(s)$ will ultimately approach zero as s increases. Furthermore, whatever is the variation in d (Reα)$/ds$ near $(m_\rho + m_N)^2$, it will approach the normal slope, ≈ 1, for sufficiently large s. Hence we have the asymptotic behavior

$$\gamma(s) \to \gamma_0(s) \to \approx \Gamma_{\text{tot}}(\infty) \quad \text{as} \quad s \to +\infty .$$

Again, taking simple functions to represent the s dependence of $\gamma_0(s)$, we have

$$\begin{aligned} \gamma_0(s) &= d_{01}(s - s_{01}), & s_{01} \lesseqgtr s \lesseqgtr s_3 \\ &= \gamma_0(s_3), & s_3 \lesseqgtr s \end{aligned} \tag{4.20}$$

with $d_{01} = 0.117$, $\gamma_0(s_3) = 0.765$, $s_{01} = (m_\pi + m_N)^2 = 1.162$, and $s_3 = 7.684$. For d (Reα)$/ds \cong 1$ when $s = m^2(S_{11}) = 2.326$, we have $\gamma_0(s) \approx \Gamma_{\text{tot}}(s) \approx 0.136$; it is reasonable to take the trajectory slope about unity as is seen in Fig. 6. The value of Γ_{tot} for $S_{11}(1.525)$ is reasonable given the present uncertainty regarding its experimental value.[6] The value of s_3, the point beyond which the γ_0 levels off, would lie between the third and fourth particle manifestations if the $S_{11}(1.525)$ trajectory had been linear. The placing of s_3 is reasonable when compared with the $D_{13}(1.52)$ trajectory and the $P_{33}(1.236)$ trajectory [see also (4.17) and (4.18)]. As regards $\gamma_\rho(s)$, we consider the simple form given below:

$$\begin{aligned} \gamma_\rho(s) &= 0, & s \lesseqgtr s_1 \\ &= d_1(s - s_1), & s_1 \lesseqgtr s \lesseqgtr s_2 \\ &= -d_{01}(s - s_3), & s_2 \lesseqgtr s \lesseqgtr s_3 \\ &= 0, & s_3 \lesseqgtr s \end{aligned} \tag{4.21}$$

where $d_1 = 16.029$, $s_1 = (m_\rho + m_N)^2 = 2.869$, $m_\rho = 0.755$, and $s_2 = (m_\rho + m_N + 0.01)^2 = 2.904$. The choice of s_2 is arbitrary; however, once chosen, d_1 has been evaluated

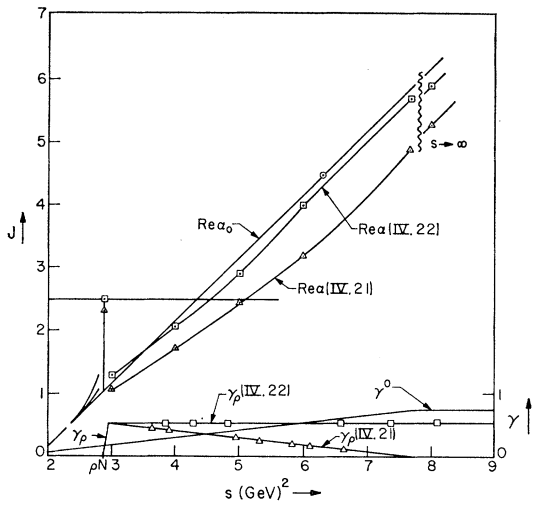

FIG. 6. Distortion caused by the sudden opening of the ρN channel on the leading S_{11} trajectory. The curve with △ shows the distorted trajectory when $\mathrm{Im}\alpha_\rho=(\sqrt{s})\gamma_\rho$ is given by Eq. (4.21). The curve with ⊡ shows the distorted trajectory when γ_ρ is given by Eq. (4.22). For the curve △, $J=2.133$ for $s=2.869$; $J=2.354$ for $s=2.886$; $J=2.163$ for $s=2.904$. For the curve ⊡, $J=2.299$ for $s=2.869$; $J=2.532$ for $s=2.886$; $J=2.348$ for $s=2.904$. The ρN threshold is given by $s=(m_\rho+m_N)^2=2.869$ for $m_\rho=0.755$. The maxima of the distortions lie between $s=2.886$ and $s=2.904$. The first spin-$\frac{5}{2}$ particle lies between $\sqrt{s}=1.694$ and $\sqrt{s}=1.704$, whereas the second spin-$\frac{5}{2}$ particle lies between $\sqrt{s}\simeq 2.12$ and $\sqrt{s}\simeq 2.26$. Energy units are in GeV.

requiring that

$$\gamma(s_2)=\gamma_0(s_2)+\gamma_\rho(s_2)=\gamma_0(s_3)\,.$$

Thus for $\gamma_\rho(s)$ given by (4.21), $\gamma(s)$ equals $\gamma_0(s)$ below the ρN threshold; near $(m_\rho+m_N)^2$ the value of $\gamma(s)$ increases rapidly, reaching and remaining at its asymptotic value for $s\geq s_2$. In (4.21), $\gamma_\rho(s)$ starts decreasing immediately beyond s_2. The decrease, of course, need not be as sudden. Hence, we also consider an extreme case of (4.21) where $\gamma_\rho(s_2)$ is kept constant and s_3 allowed to go to infinity, so that we have

$$\begin{aligned}\gamma_\rho(s)&=0, && s\leqq s_1\\ &=d_1(s-s_1), && s_1\leqq s\leqq s_2\\ &=\gamma_\rho(s_2), && s_2\leqq s.\end{aligned}\qquad(4.22)$$

The more realistic behavior of $\gamma_\rho(s)$ would be somewhere in between the two extremes (4.21) and (4.22).

The discussion of the shift arising from (4.20) will be carried out in two steps. As a first step, in (4.15), identify s_1 with s_{01} of (4.20) and $\gamma(s)$ with $\gamma_0(s)$ of (4.20) and let s_0 be suitably chosen—say, $s_0=(1.525)^2$ for simplicity, so that $\mathrm{Re}\alpha(s_0)=\alpha_0(s_0)=\frac{1}{2}$. The shift resulting from $\gamma_0(s)$ may be supposed to give rise to the normal straight-line trajectory in analogy with the $D_{13}(1.52)$ trajectory. In the next step, we identify s_1 of (4.15) with the s_1 of (4.21) or (4.22), and $\gamma(s)$ in (4.15) with $\gamma_\rho(s)$ as given by (4.21) or (4.22). The $\alpha_0(s)$ of (4.14) is now identified with the normal trajectory generated in the first step, and $s_0=(1.525)^2$ with $\mathrm{Re}\alpha(s_0)=\alpha^0(s_0)=\frac{1}{2}$ is retained for simplicity. The resulting expression for $\Delta(s)-\Delta(s_0)$ now represents the shift due to $\gamma_\rho(s)$ as given by (4.21) or (4.22). The effect of this shift is illustrated in Fig. 6. As can be seen, the distortion from the straight-line trajectory occurs primarily in the region of the ρN threshold. As the figure shows, we are faced with the distinct possibility that the trajectory passes through $J=\frac{5}{2}$ twice with a positive slope. Hence there would be two D_{15} manifestations on such a trajectory. Empirically the assignments in Tables VII and IX can be distinguished from the assignments in Table X by the presence or absence of a G_{19} resonance at $m^2=4.81$. In the last statement we are, of course, assuming a unit slope for the $D_{15}(1.68)$ trajectory of Table IX as well as presupposing that G_{19} is a sense point for this trajectory.

The mechanism for the distortion from a monotonically increasing Regge trajectory discussed above is quite general. In fact, a particle may be suspected of lying on a trajectory with a shape as in Fig. 6 if its mass is almost coincident with the threshold of a channel into which it decays primarily. As is evident, the height of the distortion depends critically upon how rapid is the increase in $\gamma(s)$ [Eq. (4.16)] as well as the magnitude of the increase.

V. CONCLUSION

In the foregoing, some dynamical ideas based on the l-excitation scheme have been presented to account for indefinitely rising Regge trajectories. In order to overcome the increasing repulsive centrifugal force, it has been suggested that the effective strength of forces due to exchanged Regge trajectories, attractive in this case, increases with energy. The output Regge trajectories would then be pulled up with energy. Viewing this in the simplest case of a single two-particle channel, we come up with the immediate conclusion that trajectories must grow at least as fast as $\sqrt{s}$. Furthermore, we have the prediction that associated with the leading output trajectory there must occur an infinite set of deeper-lying trajectories, the deeper-lying trajectories being the radial excitations of the leading trajectory. The pattern for the resonances is

$$s_n(J+2)>s_{n+1}(J)>s_n(J)\,,$$

where $s_n(J)$ represents the mass squared of a particle with spin J and radial quantum number n. For linear trajectories with unit slope, we have $s_{n+1}(J)-s_n(J)=\sqrt{2}$, in the single two-particle channel example. Empirically, the above predictions are very well satisfied for the sets where the leading trajectories are the well-established $\Delta(1.236)$ trajectory, $N(0.939)$ trajectory, and $D_{13}(1.52)$ trajectory. In the case of leading trajectories whose first manifestations have been observed, the above scheme predicts the pattern of resonances to be found.

In order to discuss the behavior of $\mathrm{Im}\alpha$, or Γ_{tot}, it is, of course, essential to consider the multichannel nature

of the problem. The simplest possiblity consistent with the above dynamical suggestion is to consider the coupling between the various channels to be weak. This assumption at once indicates that Γ_{tot} is essentially proportional to the number of two-particle channels (we have restricted our attention to such channels only) with low orbital angular momenta. In the case of trajectories linearly rising with s, it is found that the number at first increases and then reaches a constant, but finally for sufficiently large s the required two-particle channels are no longer kinematically possible. The first two stages adequately account for the behavior of Γ_{tot}. The discussion suggested that the kinematically favored decays are those in which at least one of the particles is a pion. Beyond those s for which the required two-particle low-orbital-angular-momenta channels are no longer available, no firm conclusions can be drawn, the reason being that in this case the number of channels with angular momenta $l(s)$ [$l(s)\to\infty$ as $s\to\infty$] would tend to infinity also and could thereby negate the damping due to the centrifugal barrier. If this happens, Γ_{tot} may approach a finite limit or may tend to infinity. From the empirical evidence at hand, Γ_{tot} appears to be approaching a constant.

The shift of the trajectory function generated by a single two-particle channel, due to coupling with other channels, has also been discussed. In the course of this discussion we have also considered the case when the contribution from a given channel to Imα increases in a step-function-like manner. In such an event, we are faced with the interesting possibility of two particles, identical except in mass, being assigned to the same trajectory. Although such an eventuality is rather unlikely, it is of interest. The phenomenon is analogous to the Ball-Frazer mechanism for phase shifts.

If the over-all approach is appropriate, then with the simplest association of one two-particle channel with each trajectory we require nine channels, or less, to account for the observed number of trajectory sets. The next degree of complication is that we may require a set of channels with low channel spin whose "potential matrix" may be diagonalized by a matrix dependent on s and l only for large values of these parameters. In this case, too, an increase of the effective strength of forces due to the trajectory exchanges would be necessary. It seems that some such increase is required to counter the repulsive centrifugal force in those cases where an approximation by finite number of two-particle channels is valid. Consider the dynamical ideas contained in Ref. 1, where the attempt was to keep the orbital angular momentum low and pull up the trajectory by increasing the channel spin. The relevant channels are those whose thresholds lie near the resonance mass. Under such conditions, however, the discussion concerning Fig. 4 is applicable. Applied to this case, it states that because of the nonzero mass of the hadrons, channels with *finite* orbital angular momentum and thresholds near resonance mass are kinematically not possible for sufficiently large s. This result is true provided the trajectories universally increase faster than $\sqrt{s}$ as $s\to+\infty$. But if the trajectories increased at most like $\sqrt{s}$ as $s\to+\infty$, channels meeting the basic requirements of the ideas in Ref. 1 are always available.[9] But in this event we must require that $\alpha(s)$ has an essential singularity at $s=\infty$; otherwise we are faced with undesirable properties as $s\to-\infty$, $\text{Re}\alpha\sim|s|^k\cos k\pi$, $0<k\lesssim\frac{1}{2}$. If, however, we wish to retain the faster-than-$\sqrt{s}$ growth of trajectories as $s\to+\infty$, then we have to abandon either the restriction that channel thresholds be near the resonance mass, or that the orbital angular momentum be finite, or both. If the restriction on channel thresholds is removed, then an infinite number of channels is available; little is known of such a situation. If, however, the restriction on orbital angular momentum only is removed, then the repulsive force would tend to infinity. In such a situation, the study of models, e.g., potential scattering, shows that we approach the "free-particle" case, unless we counter the repulsion by an appropriate increase of attraction. The latter, of course, requires that the effective strength of the forces due to trajectory exchanges increase with energy.

Finally, we wish to state that although an increase in the effective strength of the exchanged Regge trajectories can explain high-rising trajectories, it is conceivable that beyond a certain high energy the effective strength does not increase as rapidly. In this case, the trajectories after having risen fairly high will start falling. The empirically observed behavior would thus be accounted for here also. The question whether trajectories rise indefinitely or not is then primarily a matter of internal consistency in a given formalism.

ACKNOWLEDGMENTS

The author is grateful to Professor B. M. Udgaonkar and Dr. Y. M. Gupta for discussions during his stay at the Tata Institute for Fundamental Research. He is thankful to Professor S. C. Frautschi for various encouraging discussions, as well as for critically reading the manuscript.

[9] See also R. C. Brower and J. Harte, Phys. Rev. **164**, 1841 (1967); S. Y. Chu and C. I. Tan (Ref. 1).